

## Microfluidic Image Cytometry (μFIC) Assessments of Silver Nanoparticle Cytotoxicity

Jonghoon Park and Tae Hyun Yoon \*

*Laboratory of Nanoscale Characterization and Environmental Chemistry, Department of Chemistry,  
Hanyang University, Seoul 133-791, Korea. \*E-mail: [thyoon@gmail.com](mailto:thyoon@gmail.com)  
Received September 4, 2012, Accepted September 12, 2012*

Cytotoxicity assessment of silver nanoparticles (AgNPs) was performed using MTT-based microfluidic image cytometry (μFIC). The LC<sub>50</sub> value of HeLa cells exposed to AgNPs in the microfluidic device was estimated as 46.7 mg/L, which is similar to that estimated by MTT-based IC for cells cultured in a 96 well plate (49.9 mg/L). These results confirm that the μFIC approach can produce cytotoxicity data that is reasonably well-matched with that of the conventional 96 well plate system with much higher efficiency. This μFIC method provides many benefits including ease of use and low cost, and is a more rapid *in vitro* cell based assay for AgNPs. This may aid in speeding up data acquisition in the field of nanosafety and make a significant contribution to the quantitative understanding of nanoproperty- toxicity relationships.

**Key Words :** Microfluidic image cytometry, Microfluidic device, Cytotoxicity assessment, Ag nanoparticles, Nanotoxicity

### Introduction

Due to increasing concerns regarding potential hazards to human health and the environment, toxicity assessments of manufactured nanomaterials (MNs) and related consumer products have recently received significant attention. According to the Woodrow Wilson International Center (WWIC) on-line inventory, there were more than 1300 nanotechnology consumer products involving MNs in 2011.<sup>1</sup> Moreover, this number has been quadrupled over the last 5 years, and is expected to grow to 10,000 products within a decade.<sup>1,2</sup> Silver nanoparticles (AgNPs) in particular are one of the most common MNs used for consumer nanotechnology products due to their antimicrobial properties. In March of 2011, 313 AgNP consumer products were listed in the WWIC on-line inventory, which is 55% of the 565 total consumer nanotechnology products with explicitly referenced nanomaterials.<sup>1</sup>

This dramatic increase in the number of nanotechnology consumer products could overwhelm conventional *in vitro* and *in vivo* toxicological methods and could potentially bottleneck the advancement of nanotechnology-based industry. Thus, development of automated high-throughput screening (HTS) platforms is essential in order to increase assay throughput, and reduce cost, labor, and reagent requirements. These approaches can be combined with high content analysis (HCA), which may facilitate systematic understanding of cellular interactions with nanoparticles (NPs).<sup>3</sup> The application of a high-throughput and high contents screening (HT-HCS) approach for safety assessments of numerous MNs is expected to help screen out MNs with high toxic potential in *in vivo* testing.<sup>2</sup>

The miniaturization of cell-based assays is one of the most important tasks in enhancing efficiency and reducing costs of many *in vitro* cytotoxicity assays and drug screening pro-

cesses.<sup>4,5</sup> Recently, high-density multi-well plates have been developed, significantly improving assay throughput. However, many technical issues have been raised as miniaturization has progressed, such as practical limitations in handling sub-microliter liquids in an open well system and the need for increased well-densities per plate.<sup>4</sup> Current robotics-based HTS platforms are also extremely expensive, and are not practical for the assessment of exponentially increasing numbers of MNs. Therefore, development of new screening platforms for nanotoxicity assessments with high assay throughput and reasonable experimental cost are needed, which could speed up data acquisition for the quantitative understanding of nanoproperty-toxicity relationships.<sup>2</sup>

In order to overcome issues involved with miniaturization, there has been a recent trend toward using microfluidic devices (μFD) as potential platforms for future cell-based HTS assays. These devices offer advantages such as reducing experimental costs, increasing assay throughput, and shrinking the physical dimensions of the current instruments.<sup>5-9</sup> Several promising applications of microfluidic technology for *in vitro* HTS have been reported in which various properties of cells within microfluidic channels were monitored in a single cell assay.<sup>10-13</sup>

Microfluidic image cytometry (μFIC) is a novel microfluidic approach for *in situ* cytotoxicity assessment of cells cultured and treated within microfluidic channels under a precisely controlled chemical environment. We recently reported morphology-based<sup>12</sup> and MTT absorbance-based<sup>13</sup> μFICs, in which all treatments, measurements, and analyses of adherent cells were conducted in a precisely controlled microenvironment with minimal disturbances. Using this approach, combinatorial analysis of cell death events such as mitochondrial enzyme activity and cellular morphological changes have been performed to provide a more efficient and objective way to evaluate the cell death process.

As a follow-up to our recent publications on  $\mu$ FIC, this study expands its applications to cytotoxicity assessments of NPs. MTT cell viability assays for HeLa cells exposed to  $\text{Ag}^+$  ions and AgNPs were performed in conventional 96 well plates using a microplate reader and image cytometry.  $\mu$ FIC assessments of AgNP cytotoxicity were performed and results were compared with those obtained *via* the traditional approach. Our results suggest that  $\mu$ FIC is a novel platform for cytotoxicity assessment, and that this method is applicable to NP cytotoxicity.

## Experimental

**Preparation of AgNPs.** AgNPs used in this study (SARPU-200KW, lot no. SL-112B4DD01, ABC Nanotech, Korea) were purchased from ABC Nanotech, which is one of the reference MNs suggested by the Working Party on Manufactured Nanomaterials (WPMN) of the Organisation for Economic Co-operation and Development (OECD) as a part of the international collaboration on the risk assessment of MNs. For the removal of aggregated particles, the AgNP stock solution was filtered through a 0.2  $\mu\text{m}$  syringe filter and stored at 4  $^{\circ}\text{C}$  under dark conditions. The total silver concentration was measured in an acidified solution (4% (v/v)  $\text{HNO}_3$ ) by ICP-AES (Optima-4300 DV; PerkinElmer, Waltham, MA, USA). The hydrodynamic size of AgNPs in DMEM cell culture media without phenol-red was examined using a dynamic light scattering (DLS) instrument (Qudix, scatterscope II, Seoul, Korea). The shape and size of AgNPs were measured using transmission electron microscopy (TEM, Hitachi H-7600, Tokyo, Japan).

**Design and Fabrication of  $\mu$ FD.** As shown in Figure 1(a), the microfluidic device used in this study had four main components; inlets for media and the toxicant, a concentration gradient generator (CGG), straight channels for cell culture, and an outlet. The  $\mu$ FD was made using polydimethylsiloxane (PDMS) *via* a soft lithography technique. SU-8 2150 photoresist (Microchem, Newton, MA, USA) was spin-coated and photo lithographically patterned on a silicon wafer. The patterned silicon wafer was then silanized by exposure to tridecafluoro-1,1,2,2-tetrahydrooctyl (trichlorosilane) (Sigma Aldrich, ST. Louis, MO, USA) and was positioned inside of a Petri-dish (90  $\times$  15 mm). Sylgard 184 PDMS prepolymer and a curing agent (Dow Corning, Midland, MI, USA) were mixed at a 10:1 weight ratio and poured onto the patterned silicon wafer in the petri-dish. This was then degassed in a vacuum chamber for 10 min and subsequently baked in an oven at 60  $^{\circ}\text{C}$  for 4 h. Holes for inlets and the outlet were punched out of the PDMS layer using flat-tip needles to form fluidic connection ports. The PDMS layer and glass coverslip (24  $\times$  60 mm) were treated with oxygen plasma and bonded to each other. Before use, the microfluidic device was filled with deionized water and sterilized by UV illumination for 10min. Additionally, the  $\mu$ FD was initialized with a cell culture medium and placed inside a humidified incubator (Forma Scientific, Waltham, MA, USA) at 37  $^{\circ}\text{C}$  with 5%  $\text{CO}_2$  for more than 6 h prior to

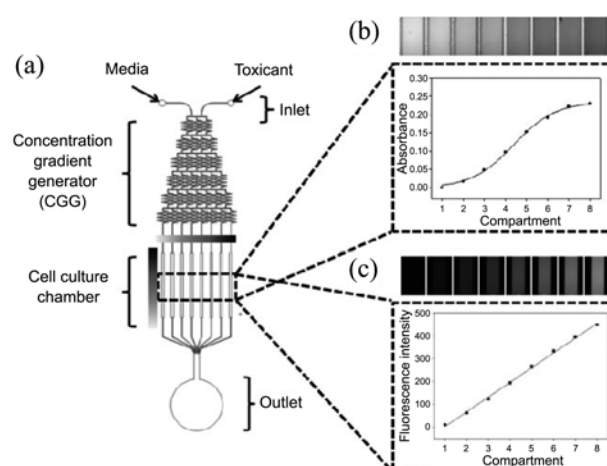


**Figure 1.** (a) Schematic illustration of the microfluidic device design. Concentration gradient profile of (b) AgNPs and (c)  $\text{Ag}^+$  ions.

cell culture experiments.

**Concentration Gradient Generation in  $\mu$ FD.** In order to confirm the concentration gradient of stable AgNPs in the microfluidic device, the AgNP suspension and distilled water were flushed through each inlet port at a rate of 1  $\mu\text{L}/\text{min}$ . Once the flow of AgNPs in the microfluidic device was stabilized, bright field optical images were acquired for each cell culture channel using an inverted type microscope (IX51, Olympus, Japan) equipped with a cooled CCD camera (RETIGA-2000RV, QImaging Ltd., Canada). The bright-field optical images obtained were further processed to develop absorbance images through an IC method. The concentration gradient of AgNPs within the microfluidics device was estimated from the absorbance values for each channel. For the confirmation of  $\text{Ag}^+$  ion concentration gradient generation, fluorescein isothiocyanate (FITC, Sigma-Aldrich, USA) was also used to estimate concentration gradient profiles from the fluorescence intensities of each channel.

**Cell Culture and AgNPs Exposure in  $\mu$ FD.** The HeLa cell line was obtained from the Korea Biological Resource Center (KBRC). Cells were cultured in fresh DMEM media (Gibco, Grand Island, NY, USA) including 10% fetal bovine serum (Gibco) and 1% penicillin-streptomycin (Gibco). Cell suspensions prepared at a concentration of  $10^4$ - $10^5$  cells/mL were loaded into the microfluidics device. The microfluidics device was then placed in a humidified incubator (Forma Scientific, Waltham, MA, USA) at 37  $^{\circ}\text{C}$  with 5%  $\text{CO}_2$  for 24 and 36 h. This cell culture cycle was repeated several times until the appropriate number of cells was obtained within the  $\mu$ FD. Solutions of  $\text{Ag}^+$  ions or AgNPs in cell culture media were then loaded into a syringe pump and were continuously exposed to cultured cells inside the microfluidic channels. One inlet was supplied with the cell culture medium, while another inlet was supplied with the AgNP suspension (100 mg/L). A concentration gradient of AgNPs (0-100 mg/L) was generated within the CGG, and adherent cells in each straight cell culture channel were exposed to different concentrations of  $\text{Ag}^+$  ions or AgNPs under continuous flow conditions for 12 h inside of the

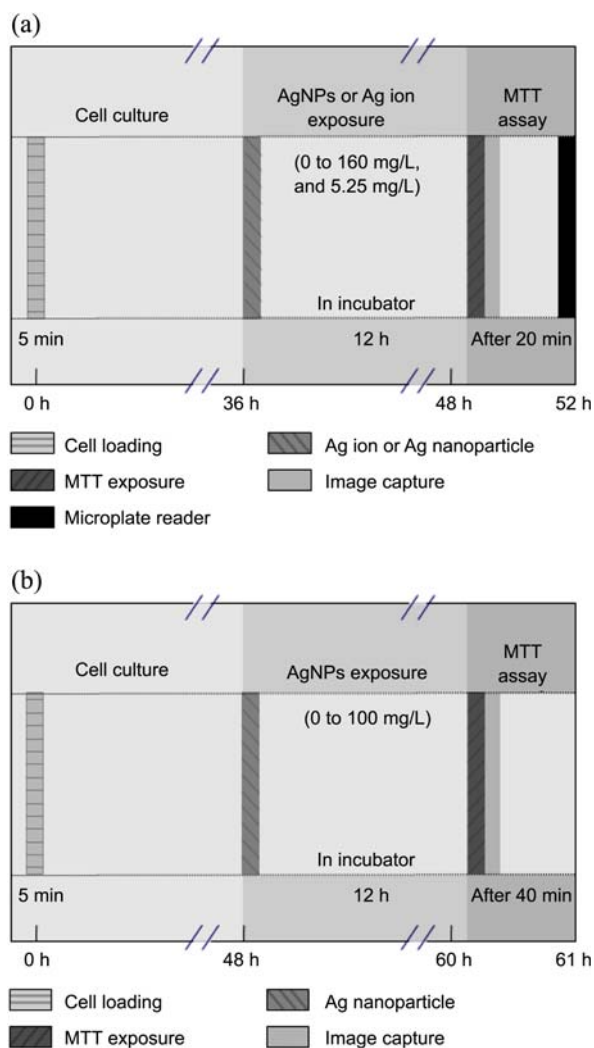


**Figure 2.** Schematic diagrams of the (a) conventional MTT protocol (in a 96 well plate), and the (b) modified MTT assay protocol for the  $\mu$ FIC-based approach.

humidified incubator (37 °C, 5% CO<sub>2</sub>).

**Conventional and Modified MTT Assays.** The MTT assay protocol was performed to assess the viability of cells exposed to Ag<sup>+</sup> ions and AgNPs. In MTT assays performed on 96 well plates, 100  $\mu$ L of Ag<sup>+</sup> ions or AgNPs in cell culture media was loaded onto the cultured HeLa cells at concentrations ranging from 0 to 5.25 mg/L (Ag<sup>+</sup> ions) and 0 to 160 mg/L (AgNPs). The 96 well plate was then placed inside of a humidified incubator at 37 °C with 5% CO<sub>2</sub> for 12 h. After removal of the media from each well, 100  $\mu$ L of 5 mg/mL MTT (Sigma Aldrich, St. Louis, MO, USA) solution in cell culture media was added to each well. Cells were again incubated at 37 °C with 5% CO<sub>2</sub> for 4 h. After incubation with the MTT solution and removal from each well, 200  $\mu$ L of DMSO solution was added to each well to dissolve the formazan crystals. Within 20 min, absorbance from dissolved MTT formazan at a wavelength of 595 nm was measured by the microplate reader (Multiskan Ex, Thermo Scientific, Waltham, MA, USA). Cell viability was expressed as the absorbance ratio between the cells exposed to Ag<sup>+</sup> ions or

AgNPs and the untreated cells.

**IC Method for  $\mu$ FIC Assessment of Cytotoxicity.** Morphological and MTT absorbance based image cytometric analyses were performed for quantification of cell death. The bright field optical images were processed to obtain formazan absorbance images, and then analyzed for cellular information. The bright field optical images were converted to corresponding optical density images by taking the logarithm of each bright-field image ( $I_1$ ) divided by a mean value ( $I_0$ ) of an area on the sample at which no absorption in this wavelength range was observed (e.g., PDMS only region). Through analyzed absorbance images, the morphological and MTT formazan absorbance information for each cell (e.g., cell circularity, cell area, mean integrated absorbance of the individual cell) were extracted using java-based image processing and analysis software (ImageJ 1.41n, NIH, USA). ImageJ macro was used for automated processing of multiple images obtained from each channel. Functions including cell segmentation, bright-field to absorbance image transformation, and cellular information measurement were applied to extract cellular information from each optical image. Segmentation of the cellular area was performed on bright-field images to obtain a ROI (region of interest), absorbance images were obtained from each bright-field image, and finally ROIs were applied to absorbance images to extract information (e.g., mean and integrated cellular absorbance) from each cell.

## Results and Discussion

In order to test the feasibility of  $\mu$ FIC for the cytotoxicity assessment of AgNPs, the following experiments were performed; 1) characterization of AgNPs and their concentration gradient in  $\mu$ FD, 2) verification of the MTT-based IC approach for cells exposed to Ag<sup>+</sup> ions in a 96 well plate, and 3) verification of the MTT-based  $\mu$ FIC approach for cells exposed to AgNPs in  $\mu$ FD.

**Characterization of AgNP and its Concentration Gradient Profile in  $\mu$ FD.** AgNPs used in this study had an average hydrodynamic size of 33.8 nm in DMEM media. Analysis of representative TEM images containing 229 particles was also performed to obtain the core size distribution, which on average was  $8.3 \pm 1.5$  nm with a nearly spherical shape. Toxicants and media injected through the two inlets were mixed inside the concentration gradient generator (CGG).<sup>14</sup> In this study, the concentration gradient of Ag<sup>+</sup> ions was generated using laminar flow and diffusional mixing within the CGG. Ag<sup>+</sup> ion concentrations were estimated at each channel from the previously measured fluorescence intensity profile of FITC, which had a comparable molecular weight and diffusion coefficient to Ag<sup>+</sup> ions. As shown in Figure 1(c), the concentration gradient of FITC was found to be linear in shape at the end of the CGG. The concentration gradient profile of AgNPs inside the microfluidic device, however, could not be estimated from the fluorescence intensity profile of small molecules (e.g., FITC), since the AgNPs have much higher mass per particle and consequently a

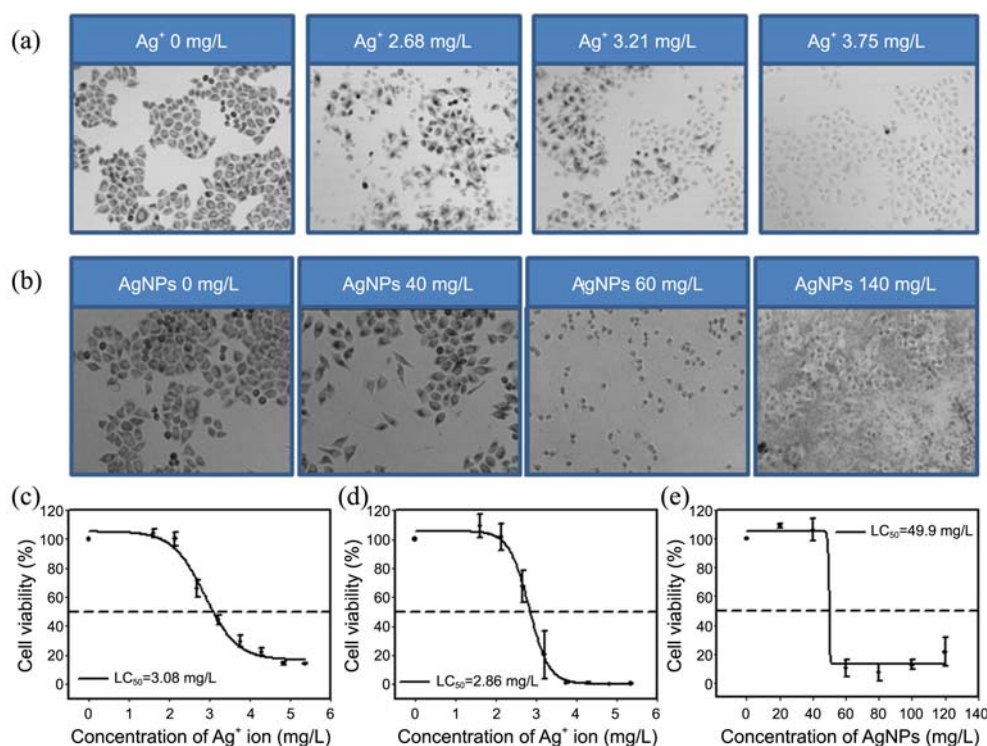


**Figure 3.** Optical images of HeLa cells exposed to various concentrations of (a)  $\text{Ag}^+$  ions and (b) AgNPs in 96 well plates. MTT cell viability curves for HeLa cells cultured in 96 well plates and exposed to (c)  $\text{Ag}^+$  ions measured by a microplate reader, and (d)  $\text{Ag}^+$  ions and (e) AgNPs measured by image cytometry.

much slower diffusion rate. Therefore, the concentration profile of AgNPs was directly measured from the optical density profile in the microfluidic device. By acquiring and analyzing bright-field optical images, we were able to clearly observe profiles of the AgNP gradient, which was found to form an 'S' shaped curve at the end of the CGG (see Figure 1(b)).

**Validation of the MTT-based IC Approach.** Recently, the MTT-based IC approach has been applied to cytotoxicity assessments of  $\text{Cd}^{2+}$ .<sup>13</sup> This alternative approach has helped us to improve on traditional assay throughput by simplifying the protocol and reducing the time required for the viability assay. Here, mitochondrial enzyme activity (MEA) was used to quantify cell death as an endpoint of apoptosis, and "cellular absorbance" values of each cell were obtained *via* image analysis. Cell viabilities in each sample were measured as the percentage of cells with high cellular absorbance. Based on these values, we calculated a viability curve for HeLa cells exposed to  $\text{Ag}^+$  ions and AgNPs as well as an  $\text{LC}_{50}$  value for both  $\text{Ag}^+$  ions and AgNPs.

Viability curves and  $\text{LC}_{50}$  values of cells exposed to  $\text{Ag}^+$  ions shown in Figure 3(c) and (d) were obtained using a conventional microplate reader and an MTT-based IC approach. The  $\text{LC}_{50}$  values estimated from both methods were 3.08 mg/L, and 2.86 mg/L, respectively, which confirmed that the MTT-based IC approach used in this study is compatible with conventional MTT methods and may be used for cytotoxicity assessment of toxic chemicals in  $\mu\text{FD}$  including AgNPs.

**Application of MTT-based  $\mu\text{FIC}$  for the Cytotoxicity Assessment of AgNP.** In Figure 4(a), optical images of HeLa cells exposed to 0.0 (channel #1), 41.4 (channel #4) and 100.0 mg/L (channel #8) AgNPs in  $\mu\text{FD}$  are presented. Cell shrinkage and cellular absorbance reduction were observed with increasing AgNP concentration (Figure 4(a) and (b)). Additionally, the viability curve and  $\text{LC}_{50}$  value of these cells are presented in Figure 4(c). The  $\text{LC}_{50}$  value estimated from the  $\mu\text{FIC}$  approach was 46.7 mg/L, which was similar to that estimated by MTT-based IC for cells cultured in a 96 well plate (49.9 mg/L, Figure 3(e)). These results suggest that the  $\mu\text{FIC}$  experiments performed in the microfluidics device with analysis conducted *via* image cytometry may produce cytotoxicity data that are comparable to the conventional 96 well plate system with a much higher efficiency. Therefore, this novel approach may make significant contributions to cytotoxicity assessments of NPs with high assay throughput, which could speed up data acquisition for the quantitative understanding of nanoproperty-toxicity relationships.

## Conclusion

Here, we have demonstrated a novel cytotoxicity assessment method involving a microfluidic device and image cytometric approach (*i.e.*,  $\mu\text{FIC}$ ), which have many benefits including ease of use and low cost, and constitute a more rapid *in vitro* cell based assay for AgNPs. This type of HT-HCS approach can help to speed up data acquisition in the

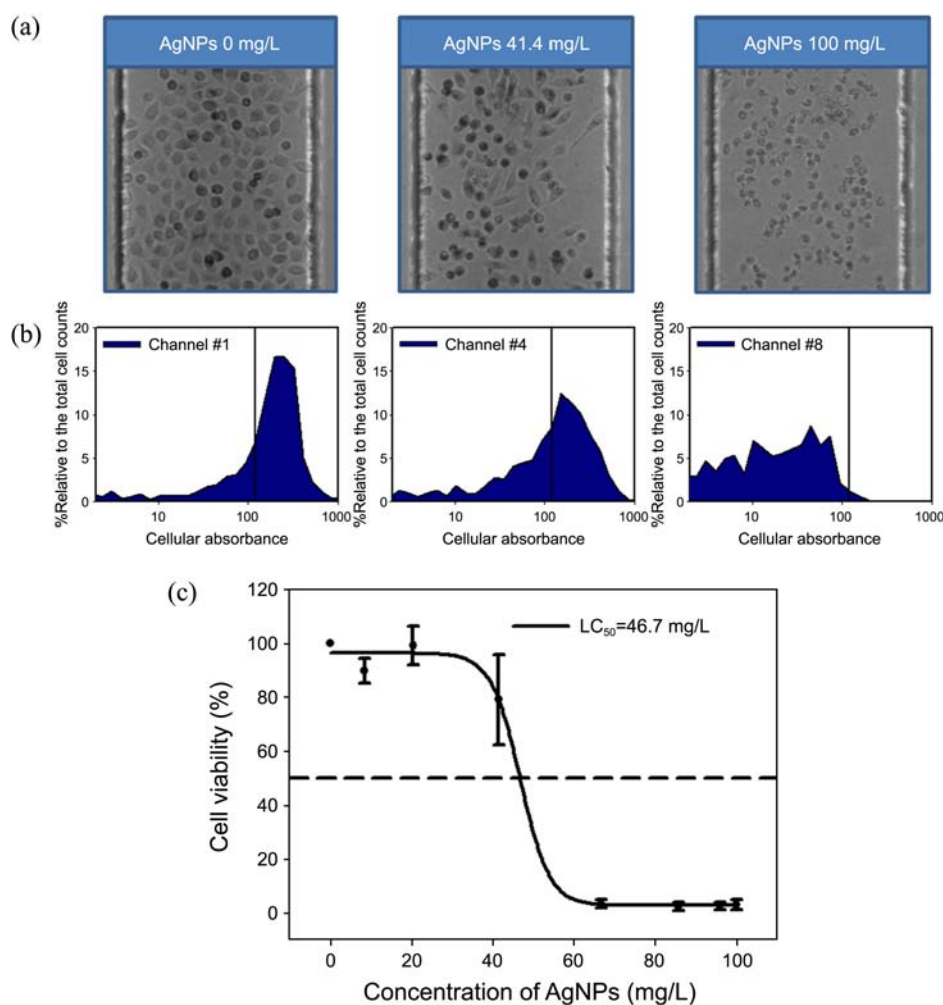


**Figure 4.** (a) Optical images of HeLa cells cultured and exposed to AgNPs within the microfluidic device. (b) Histogram of integrated cellular absorbances for the microfluidic channels shown in (a). (c)  $\mu$ FIC-based MTT cell viability curve for HeLa cells cultured and exposed to AgNPs within the microfluidic device.

field of nanosafety, and will make a significant contribution to the quantitative understanding of nanoproperty-toxicity relationships. Additionally, the image cytometric approach adapted in this study may also help to overcome recently reported limitations of the conventional MTT viability assay by measuring only intracellularly reduced formazan.

**Acknowledgments.** This work was financially supported by the Nano R&D program through the Korea Science and Engineering Foundation (KOSEF), which was funded by the Ministry of Education, Science and Technology (MEST) (2008-02968).

## References

1. Nanotechnology Consumer Product Inventory. Washington DC: Projecton Emerging Nanotechnology. Woodrow Wilson International Center for Scholars. Available at <http://www.nanotechproject.org/inventories/consumer/>
2. George, S.; Pokhrel, S.; Xia, T.; Gilbert, B.; Ji, Z.; Schowalter, M.; Rosenauer, A.; Damoiseaux, R.; Bradley, K. A.; Madler, L.; Nel, A. E. *ACS Nano* **2010**, *4*, 15.
3. Abraham, V. C.; Taylor, D. L.; Haskins, J. R. *Trends in Biotechnology* **2004**, *22*, 15.
4. Sundberg, S. A. *Curr. Opin. Biotechnol.* **2000**, *11*, 47.
5. El-Ali, J.; Sorger, P. K.; Jensen, K. F. *Nature* **2006**, *442*, 403.
6. Ye, N. N.; Qin, J. H.; Shi, W. W.; Liu, X.; Lin, B. C. *Lab Chip* **2007**, *7*, 1696.
7. Ye, N. N.; Qin, J. H.; Shi, W. W.; Lin, B. C. *Electrophoresis* **2007**, *28*, 1146.
8. Siyan, W.; Feng, Y.; Lichuan, Z.; Jiarui, W.; Yingyan, W.; Li, J.; Bingcheng, L.; Qi, W. *J. Pharm. Biomed. Anal.* **2009**, *49*, 806.
9. Mahto, S. K.; Yoon, T. H.; Shin, H.; Rhee, S. W. *Biomed. Micro-devices* **2009**, *11*, 401.
10. Hirono, T.; Arimoto, H.; Okawa, S.; Yamada, Y. *Meas. Sci. & Technol.* **2008**, *19*, 025401.
11. Cheong, R.; Wang, C. J.; Levchenko, A. *Sci. Signaling* **2009**, *2*, pl2.
12. Kim, M. J.; Lim, K. H.; Yoo, H. J.; Yoon, T. H. *Lab Chip* **2010**, *10*, 415.
13. Lim, K. H.; Park, J.; Rhee, S. W.; Yoon, T. H. *Cytom. Part A* **2012**, *81A*, 691.
14. Dertinger, S. K. W.; Chiu, D. T.; Jeon, N. L.; Whitesides, G. M. *Anal. Chem.* **2001**, *73*, 1240.